

# **Rapid room temperature syntheses of zeolitic- imidazolate frameworks (ZIFs) nanocrystals**

---

## **Supplementary information**

Min Tu, Christian Wiktor, Christoph Rösler and Roland A. Fischer\*

Chair of Inorganic Chemistry II-Organometallics and Materials Chemistry  
Ruhr University Bochum, D-44780 Bochum, Germany

## 1 Materials

Zn(NO<sub>3</sub>)<sub>2</sub>·6H<sub>2</sub>O (98%) was purchased from J. T. Baker. Zn(CH<sub>3</sub>COO)<sub>2</sub>·2H<sub>2</sub>O (98%) and benzimidazole (bIm, 98%) were purchased from Arcos Organics. 2-nitroimidazole (nIm, 98%), 4,5-dichloroimidazole (dcIm, 98%) were purchased from ABCR. Methanol (99.9%) was purchased from VWR. N,N-dimethylformamide (DMF, 99.99%) was purchased from Fischer Chemical. All the chemicals were used without further purification.

## 2 General methods

The powder ZIF samples were dropped onto a zero background silicon wafer for powder X-ray diffraction (PXRD) measurements on the X'Pert PRO PANalytical equipment (Bragg-Brentano geometry with automatic divergence slits, position sensitive detector, continuous mode, room temperature, Cu-K $\alpha$  radiation, Ni filter, the range of  $2\theta = 5\text{--}30^\circ$ , at a step of  $0.0197^\circ$ , with accumulation time 200s per step). Bright field transmission electron microscope (BFTEM) images were recorded on a Tecnai G<sup>2</sup> F20 equipped with a Schottky field emission gun operated at an acceleration voltage of 200 kV. The size distributions were determined by measuring the projected areas of nano ZIF crystals in BFTEM images. The projected area was transformed into the "diameter" of the crystals by assuming aspherical shape for them. Scanning electron microscope (SEM) images were recorded on a LEO1530 Gemini FESEM or FEI ESEM Dual Beam™ Quanta 3D FEG microscope. Dynamic light scattering (DLS) measurements were performed on a Zetasizer Nano ZS from Malvern instrument equipped with a He-Ne laser ( $\lambda = 632.8$  nm) in the backscattering detection mode. The obtained data was analyzed by dispersion technology software program. TGA measurements were performed on a Seiko TG/DTA 6300S11 instrument (sample weight approximately 10 mg) at a heating rate of 5 °C/min in the range from 30 to 800 °C under nitrogen (99.999%). IR spectra were recorded inside a glovebox on a Bruker Alpha-P FTIR instrument in the ATR geometry with a diamond ATR unit. The N<sub>2</sub> and CO<sub>2</sub> sorption measurements were performed at 77 K and 195K, respectively, by using a Quantachrome Autosorp-1 MP instrument and optimized

protocols and gases of 99.9995 % purity. The detection of methanol vapor on ZIF/QCM devices was performed on environment controlled QCM equipment according to previous reported procedure.<sup>1</sup>

### **3 Synthesis procedures**

#### **3.1 Synthesis of ZIF-7 nanocrystals**

136 mg  $\text{Zn}(\text{NO}_3)_2 \cdot 6\text{H}_2\text{O}$  ( 0.5 mmol) was dissolved in 5 ml DMF, and 120 mg bIm (1 mmol) was dissolved in 5 ml methanol. After complete dissolved,  $\text{Zn}(\text{NO}_3)_2 \cdot 6\text{H}_2\text{O}$  DMF solution was poured into bIm methanol solution quickly. The mixture slowly became turbid and stirring continued up to ca. 30 min, the as-synthesized ZIF-7 was collected by centrifugation (7800 rpm, 1.5 h). The yield of ZIF-7 nanocrystals was ~78% based on zinc.

#### **3.2 Synthesis of ZIF-65-Zn nanocrystals**

110 mg  $\text{Zn}(\text{CH}_3\text{COO})_2 \cdot 2\text{H}_2\text{O}$  ( 0.5 mmol) was dissolved in 5 ml DMF, and 113 mg nIm (1 mmol) was dissolved in 5 ml methanol. After complete dissolved,  $\text{Zn}(\text{CH}_3\text{COO})_2 \cdot 2\text{H}_2\text{O}$  DMF solution was poured into nIm methanol solution quickly. The mixture became milky immediately and stirring continued. After ca. 30 min, the as-synthesized ZIF-65-Zn was collected by centrifugation (7800 rpm, 1.5 h). The yield of ZIF-65-Zn nanocrystals was ~90% based on zinc.

#### **3.3 Synthesis of ZIF-71 nanocrystals**

In the case of synthesis of ZIF-71 nanocrystals, 110 mg  $\text{Zn}(\text{CH}_3\text{COO})_2 \cdot 2\text{H}_2\text{O}$  ( 0.5 mmol) was dissolved in 5 ml DMF, and 160 mg dcIm (1 mmol) was dissolved in 5 ml methanol. After complete dissolved,  $\text{Zn}(\text{CH}_3\text{COO})_2 \cdot 2\text{H}_2\text{O}$  DMF solution was poured into dcIm methanol solution quickly. The mixture became milky immediately and stirring continued up to ca. 30 min, then the as-synthesized ZIF-71 was collected by centrifugation (7800 rpm, 1.5 h). The yield of ZIF-71 nanocrystals was ~81% based on zinc.

After collect the samples by centrifugation, they were washed with methanol by 3 repetitions of sonication-centrifugation cycles to remove the unreacted chemicals. Afterwards, the obtained nanocrystals were dried at 60 °C overnight, and activate at 180 °C under reduced pressure, and then stored in a glovebox for further measurements (PXRD, IR and BET). The yields of them were calculated based on the weight after activation.

#### 4 Supplementary figures and tables

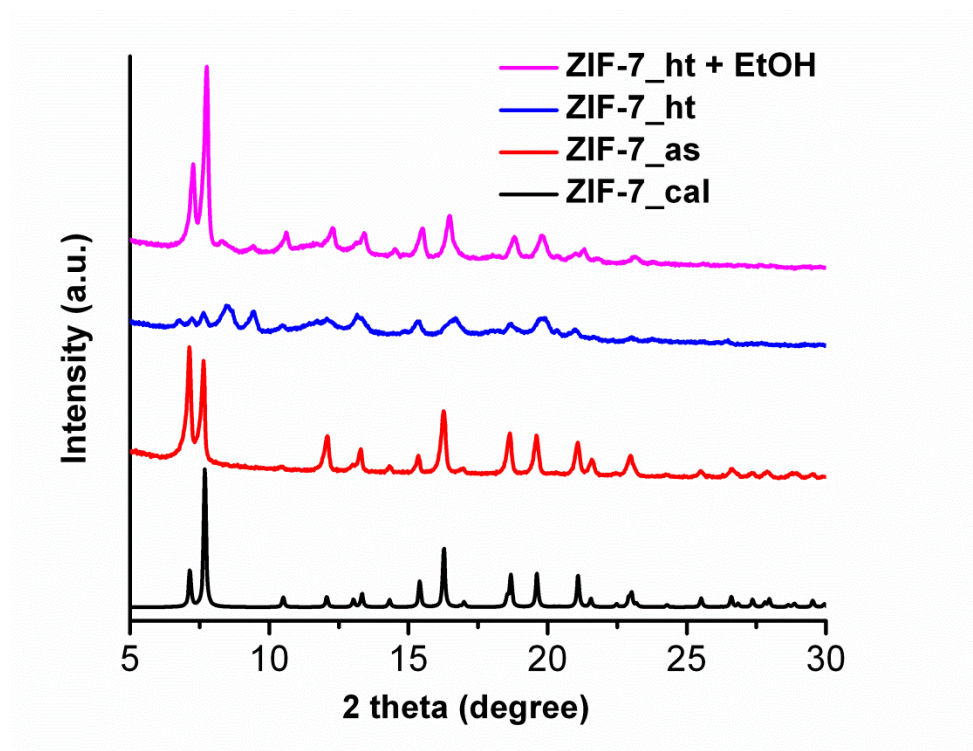


Figure S1 PXRD patterns of simulated, as-synthesized, activated ZIF-7 and the activated ZIF-7 after exposure to ethanol vapor for 1day at room temperature. As shown in this figure, the PXRD pattern of as-synthesized ZIF-7 matches well with the calculated one. However, the structure transformed from its large pore phase to the narrow pore phase, which is consistent to the previous report.<sup>2, 3</sup> Interestingly, the narrow pore phase can be transformed back to its large pore phase after exposure in ethanol vapor for one day, demonstrating the high flexibility and reversible structure change upon guest loading and removal.

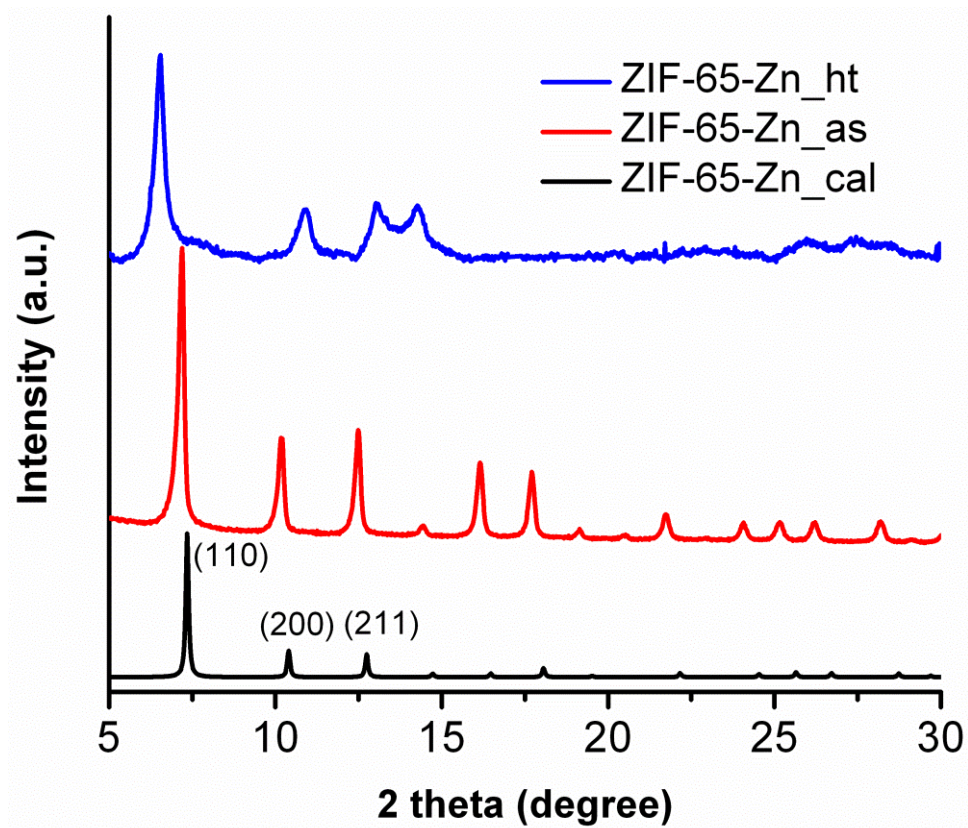


Figure S2 PXRD patterns of as-synthesized and activated ZIF-65-Zn nanocrystals in comparison with the simulated pattern. As shown in this figure, the PXRD pattern of as-synthesized ZIF-65-Zn matches with the calculated one. After removal of guest molecules, the structure transformed to another phase which we cannot solve at this moment.

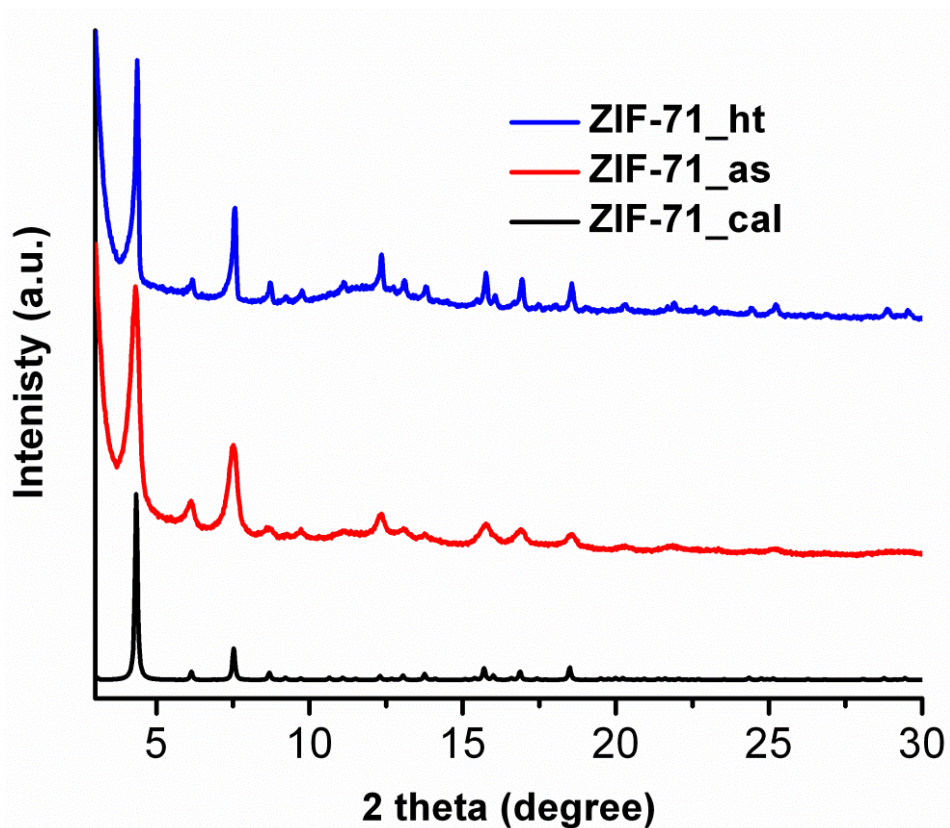


Figure S3 PXRD patterns of as-synthesized and activated ZIF-71 nanocrystals in comparison with the simulated pattern. As seen from this figure, no structure changes could be observed after activation at 180 °C under reduced pressure. However, the reflection of activated ZIF-71 samples became narrower compared to the as-synthesized one. This is possibly due to the reaction of Zn(dcIm) moieties at the surfaces during drying and activation step resulting in the formation of strong covalent Zn-dcIm-Zn linkers between different nanocrystals.

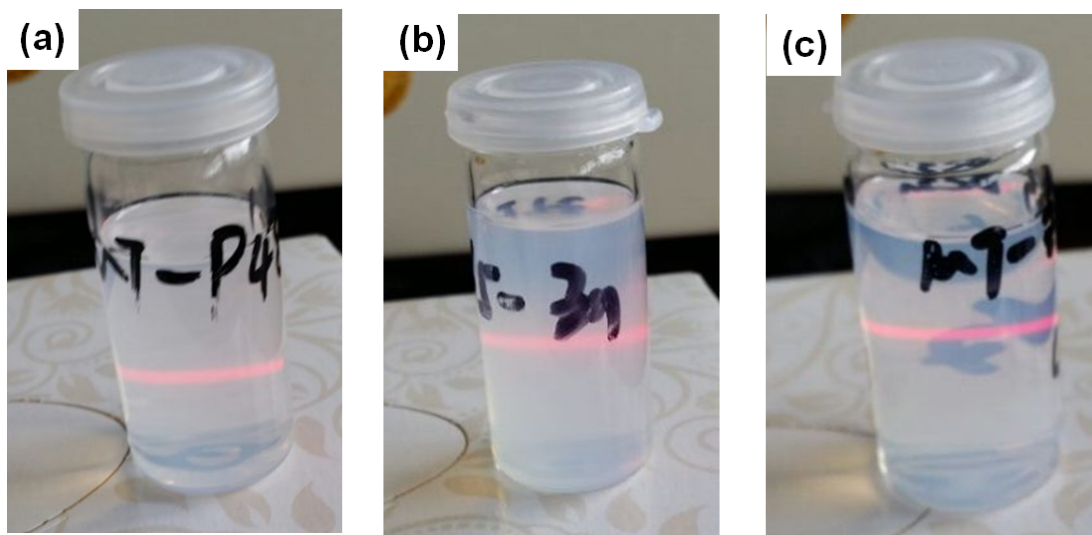


Figure S4 Photographs of stable ZIF-7 (a), ZIF-65-Zn (b) and ZIF-71 (c) dispersions in ethanol while demonstrating the Tyndall effect with a laser pointer.

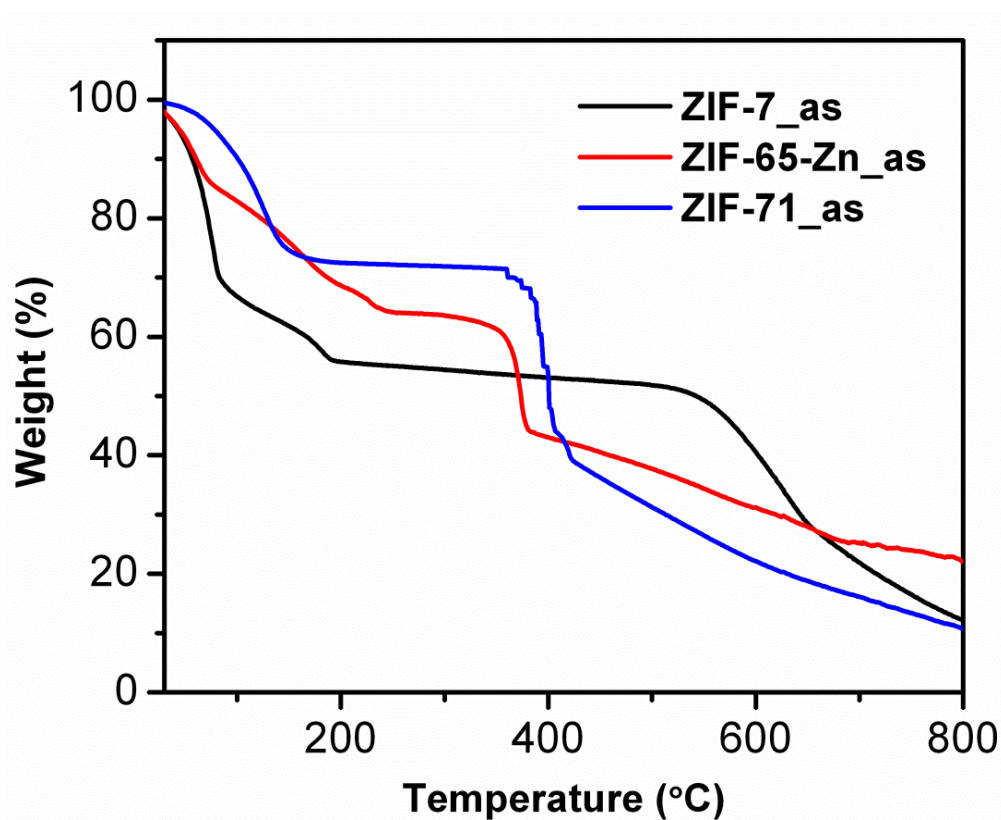


Figure S5 TGA curves of as-synthesized ZIF-7, ZIF-65-Zn and ZIF-71 nanocrystals.

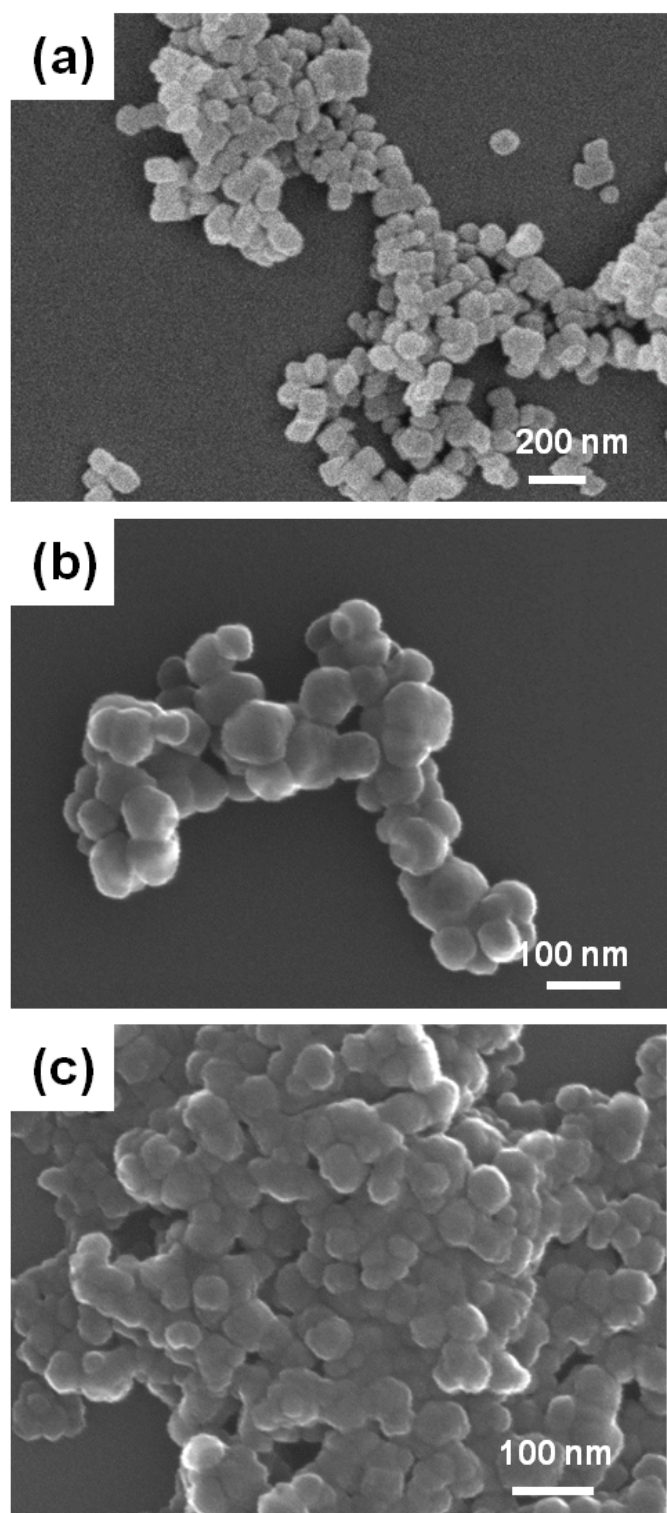


Figure S6 SEM images of nanosized ZIF-7 (a), ZIF-65-Zn (b) and ZIF-71 (c).



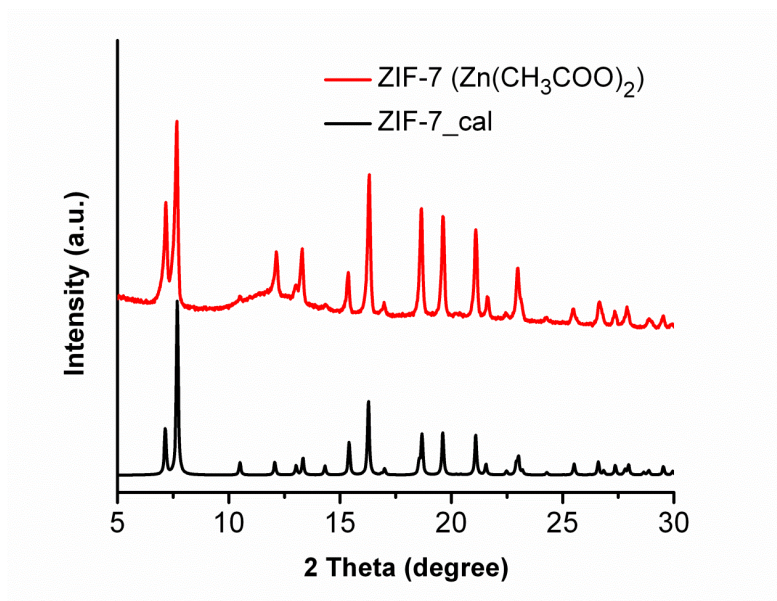


Figure S7 PXRD patterns of ZIF-7 synthesized using  $\text{Zn}(\text{CH}_3\text{COO})_2 \cdot 2\text{H}_2\text{O}$  as zinc source.

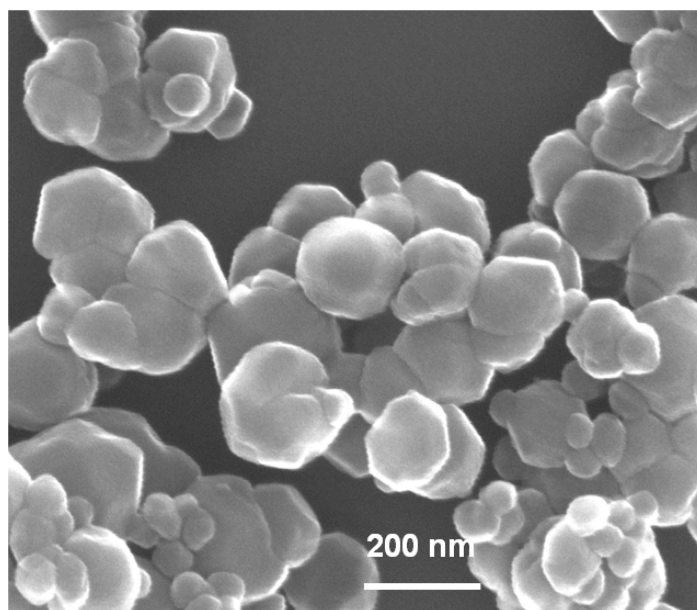


Figure S8 SEM image of ZIF-7 synthesized using  $\text{Zn}(\text{CH}_3\text{COO})_2 \cdot 2\text{H}_2\text{O}$  as zinc source.

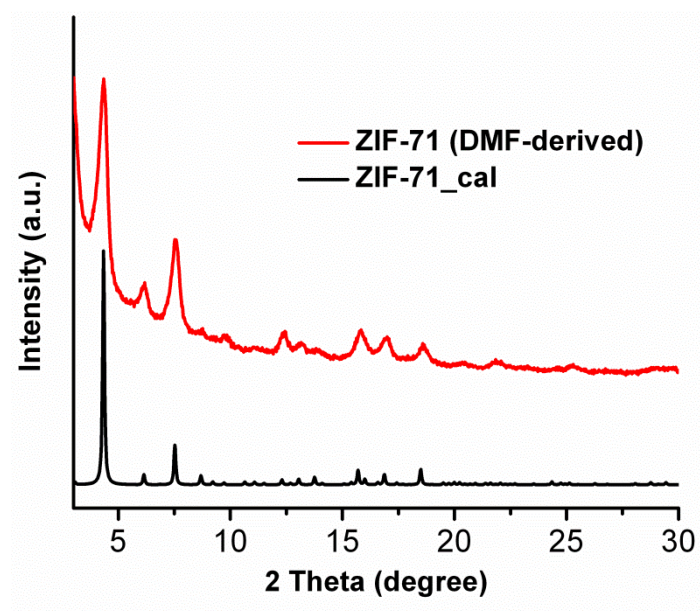


Figure S9 PXRD patterns of ZIF-71 synthesized in DMF and calculated ZIF-71

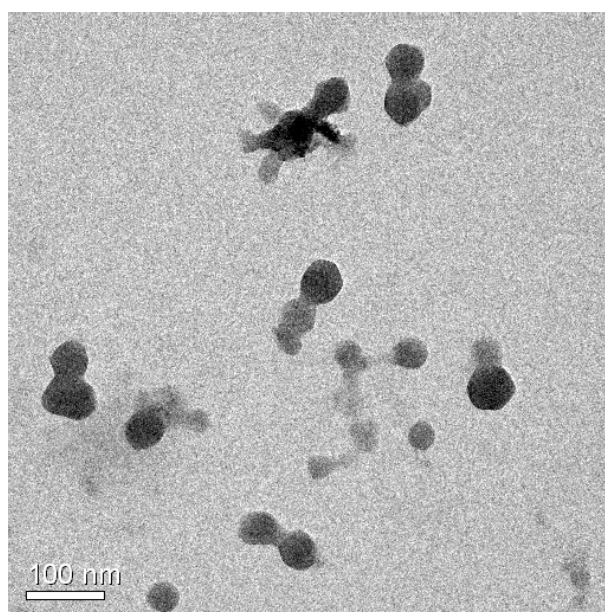


Figure S10 TEM image of ZIF-71 synthesized in DMF system.

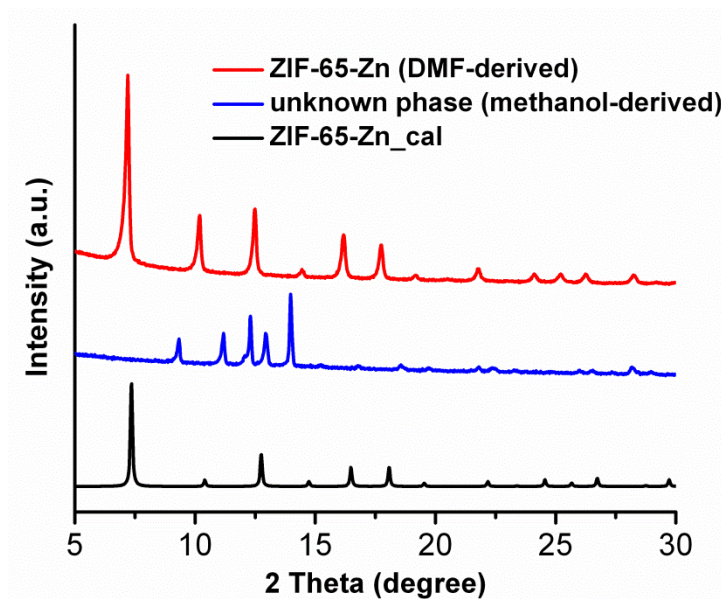


Figure S11 PXRD patterns of ZIF-65-Zn synthesized in DMF and calculated ZIF-65-Zn. An unknown phase was obtained from methanol system.

Table S1 Investigation of solvent effects on syntheses of ZIFs

	DMF	MeOH	DMF:MeOH=1:1
<b>ZIF-7</b>	30 nm <sup>4</sup>	amorphous	~112 nm
<b>ZIF-65-Zn</b>	microcrystal	unknown phase	~125 nm
<b>ZIF-71</b>	~55 nm	microcrystal <sup>5</sup>	~83 nm

Table S2 Investigation of the effects of metal source on syntheses of ZIFs

	Zn(NO <sub>3</sub> ) <sub>2</sub> ·6H <sub>2</sub> O	Zn(CH <sub>3</sub> COO) <sub>2</sub> ·2H <sub>2</sub> O
<b>ZIF-7</b>	~112 nm	~200 nm
<b>ZIF-65-Zn</b>	clear solution	~125 nm
<b>ZIF-71</b>	clear solution	~83 nm

1. M. Tu and R. A. Fischer, *Journal of Materials Chemistry A*, 2014, **2**, 2018-2022.
2. P. Zhao, G. I. Lampronti, G. O. Lloyd, E. Suard and S. A. T. Redfern, *Journal of Materials Chemistry A*, 2014, **2**, 620-623.
3. S. Aguado, G. Bergeret, M. P. Titus, V. Moizan, C. Nieto-Draghi, N. Bats and D. Farrusseng, *New Journal of Chemistry*, 2011, **35**, 546-550.
4. Y.-S. Li, H. Bux, A. Feldhoff, G.-L. Li, W.-S. Yang and J. Caro, *Advanced Materials*, 2010, **22**, 3322-3326.
5. R. P. Lively, M. E. Dose, J. A. Thompson, B. A. McCool, R. R. Chance and W. J. Koros, *Chemical Communications*, 2011, **47**, 8667-8669.